Journal of Cleaner Production 362 (2022) 132389

Contents lists available at ScienceDirect

Journal of Cleaner Production

journal homepage: www.elsevier.com/locate/jclepro

# Maximising the valorisation of organic waste locally available via carbon-to-nitrogen ratio Supply Composite Curve shifting

Wan Choy Chee [a], Wai Shin Ho [a,*], Angel Xin Yee Mah [b], Jiří Jaromír Klemeš [c], Yee Van Fan [c], Cassendra Phun Chien Bong [a], Keng Yinn Wong [a,d], Haslenda Hashim [a], Sharifah Rafidah Wan Alwi [a], Zarina Muis [a]

[a] Process Systems Engineering Centre (PROSPECT), Faculty of Chemical Engineering, Universiti Teknologi Malaysia, 81310 Skudai, Johor, Malaysia
[b] NUS Environmental Research Institute, National University of Singapore, 1 Create Way, Create Tower #15-02, 138602, Singapore
[c] Sustainable Process Integration Laboratory – SPIL, NETME Centre, Faculty of Mechanical Engineering, Brno University of Technology - VUT Brno, Technická 2896/2, 616 69, Brno, Czech Republic
[d] School of Mechanical Engineering, Faculty of Engineering, Universiti Teknologi Malaysia, 81310 Skudai, Johor, Malaysia

ARTICLE INFO

Handling Editor: Cecilia Maria Villas Bôas de Almeida

ABSTRACT

Valorisation of organic waste can lead to cleaner production in the energy sector. One factor affecting the decision for organic waste valorisation to value-added products through biological processes is the carbon-to-nitrogen (C/N) ratio. All biological processes have preferential C/N ratios for optimum performance, while organic waste comes with a wide range of C/N ratios. The mismatch of the C/N ratio between the supply stream (organic waste) and the demand stream (biological process) can lead to suboptimal process performance and affect resource allocation. In this study, a new graphical C/N ratio Pinch Analysis approach was proposed by plotting cumulative carbon mass flowrate versus the cumulative nitrogen mass flowrate as x- and y-axes for the supply and demand sides. A series of graphical Supply Composite Curve (SCC) shifting, namely SCC right-shifting, SCC end-shifting, SCC detaching, and SCC down-shifting, were developed explicitly tackling different supply stream conditions in the hypothetical case studies while satisfying the demand streams with the aid of external supply. The external supply was determined by filling the gaps formed after the SCC was shifted to the right of the Demand Composite Curve (DCC). Specific heuristics were established to assess the range of C/N ratio for the external supply that is eligible and preferred to satisfy the demand streams. Stepwise procedures for mass flowrate allocation to mix the supply and match the demand were introduced. In this study, the demands for Case Study 1 were satisfied by 59.15% OWLA with 40.83% ES 3. For Case Study 2, the demands were satisfied by 76.19% OWLA with 23.81% ES 1. For Case Study 3, the demands were satisfied by 91.54% OWLA with 8.46% ES 1. The integration of the C/N ratio element in the Pinch-based Analysis of SCC shifting and exploring new optimisation scope can act as an advising tool for any individual, party, or organisation to optimally valorise the organic waste found within a local region.

## 1. Background

Organic waste has been disposed of across various sectors worldwide, such as from industrial, commercial and residential sectors to open landfills. The release of landfill gases such as methane and non-methane organic compounds contributes to the greenhouse effect. Also, methane is 80 times more potent than carbon dioxide at heating the earth in the first 20 y after it is released into the atmosphere (Black et al., 2021). Recently, the research on sustainable biofuels, such as methane, ethanol and hydrogen, has become a trending topic due to the continual depletion of conventional resources. These biofuels can be produced from organic waste via biological processes, for example, bioethanol fermentation and anaerobic digestion for biomethane. Nevertheless, each organic waste has its unique carbon-to-nitrogen (C/N) ratio and mass flowrate availability. At the same time, each biological processes have its own preferred C/N ratio for optimum production. These lead to the varied suitability of different organic waste for different bio-processes. C/N ratio is one of the essential parameters affecting the

* Corresponding author.
E-mail address: hwshin@utm.my (W.S. Ho).

https://doi.org/10.1016/j.jclepro.2022.132389
Received 19 February 2022; Received in revised form 12 May 2022; Accepted 23 May 2022
Available online 30 May 2022
0959-6526/

conversion rate of organic waste to products in bioprocesses. It serves as an indicator of nutrient availability, either supporting or limiting microbial activity. The incompatibility of the C/N ratio among the supply and demand becomes a concern when valorising the organic waste to produce biofuels. The availability of organic waste, as well as the mass flowrate required for biofuel generation, makes organic waste valorisation more complicated.

This research focuses on the mass flowrate allocation of carbon and nitrogen components in terms of the C/N ratio from organic waste available to designated biofuels through various bioprocesses. On the supply side, the C/N ratio is defined as the total mass of carbon against nitrogen components found within the organic waste. On the demand side, the C/N ratio is referred to as the parameter required by the bioprocesses. The bioprocesses governed by the microbial community are C/N ratio sensitive, in which proper resources mixing, matching, and allocation are crucial to optimise the productivity of the value-added product. During the mix and match and allocation of resources, organic waste acts as the supply source, and bioprocesses serve as demand for carbon and nitrogen.

The main objective of this paper is to develop a C/N ratio Pinch Analysis for an optimal allocation between organic waste (i.e. supply) and bioprocesses (i.e. demand). The Pinch-based analysis developed in this study is tailored to the C/N ratio and mass flowrate of the supply and demand streams in selected bioprocesses, including anaerobic digestion for biomethane production and biohydrogen fermentation and bioethanol fermentation. In contrast to traditional Pinch approaches, local organic waste resources management strategy is frequently implemented using an optimisation tool that is optimised using a "black-box" mathematical model (Juul et al., 2013). A visual approach based on thermodynamics like SCC shifting based on Pinch Analysis allows for better comprehension of the decision-making process. The methodology and optimisation approaches were inspired by the literature mentioned previously to deal with the inconsistency issues found in organic waste. The approach is adopted from Water Pinch Analysis (WPA), where the x- and y-axes of cumulative concentration and mass flowrate (Wan Alwi and Manan, 2007) were assimilated into carbon and nitrogen mass flowrate in this study. The gradient of the curve represented in this analysis is the C/N ratio, while for the Water Pinch Analysis, the curve represents the water quality in terms of concentration of impurities. In the previous study, the designated bioprocesses were satisfied by valorising organic waste locally available with the support of external supply (Chin et al., 2021). However, the C/N ratio of the external supply was determined by drawing a straight line to seal the gap formed after the SCC shifting was performed. The external supply with a specific C/N ratio was not easy to get in real life, and in this study, several heuristics were created to determine the external supply with a C/N ratio that is eligible and preferred to satisfy the designated bioprocesses. New SCC shifted approaches, such as SCC end-shifting, SCC down-shifting, SCC right-shifting and SCC detaching, were being introduced in targeting the supply side. The plot of carbon versus nitrogen mass flowrate as the quantity parameter for the x- and y-axes of Pinch Analysis was introduced in this study, where the work has never been done before in any existing mass-based Pinch Analysis. Also, the steps to perform resource allocation for each supply stream were developed in this study. The work of resources allocation is not only required to satisfy the C/N ratio required by the demand sides, but the demanded mass flowrate for each of the designated bioprocesses also needs to be satisfied. From the aspect of academia, this study extended a new application of the Pinch Analysis concept in dealing with mass balance for bioprocesses. Also, the Pinch based method provide decision-makers with a more intuitive grasp of the planning problem and potential solutions. From the aspect of the environment, the mass flowrate allocation of organic waste resources prevents the emission of landfill gases into the atmosphere and is able to generate green and sustainable energy resources as an alternative plan for depleting conventional energy resources. The production of bioenergy by utilising organic waste as an alternative source of sustainable energy is important for industrial sustainability. By applying the SCC shifting approaches developed from this study for the valorisation of organic waste, the utilisation of organic waste locally available able to be maximised with the support of a minimum amount of external supply. This work can be useful for a party, organisation or company interested in investing in a bioenergy project and improving the waste management system.

### 1.1. C/N ratio of organic waste

The carbon involved in calculating the C/N ratio defined as the available carbon is Total Organic Carbon (TOC), a lignin-free carbon due to the non-degradable properties of lignin carbon (Hills, 1979). On the other hand, the nitrogen in the C/N ratio calculation is defined as the Total Kjeldahl Nitrogen (TKN). The action of mixing two or more substrates to obtain a synergistic effect was initially found in composting (Guo et al., 2012). It is commonly used to achieve a balanced C/N ratio required by the targeted bioprocess by mixing different waste streams of different C/N ratios. The use of co-substrate has shown a positive effect on various biological processes. For example, during anaerobic digestion, which is the degradation of organic waste to produce methane-containing biogas in the absence of oxygen, higher biogas production was observed. Shahbaz et al. (2020) concluded the co-digestion of paper waste with food waste to form a mixture with a C/N ratio of 25 was able to produce the most methane yield compared to mono digestion of paper waste, cardboard and tissue waste with a C/N ratio of 379, 355 and 188 each. Beniche et al. (2020) achieved a biodegradability of 98% while producing methane via co-digestion of food waste with agricultural waste mixtures at a C/N ratio of 45 compared to a C/N ratio of 56 (85% biodegradability). Shahbaz et al. (2019) investigated the best C/N ratio for biogas, and methane production was 20, from the range of 20–40. Guo et al. (2012) successfully co-composted pig faeces and corn stalks mixture at a C/N ratio of 18. Yong et al. (2015) found that co-digestion of food waste and straw to form a mixture at a C/N ratio of 30.9 was the best from the range 28.4–43.4 as it yields the most methane. During bioethanol fermentation, Ding et al. (2016) discovered the co-fermentation of macro-and micro-algal biomass at a C/N ratio of 20 was the best among the C/N ratio range from 20 to 26.2.

### 1.2. Pinch Analysis

Pinch Analysis was initially developed to maximise heat energy utilisation for a series of process streams and minimise external heat energy required via a thermodynamically based and graphically represented approach (Flower and Linnhoff, 1979). The fundamentals behind the Pinch Analysis process synthesis and optimisation are mass and energy balances (Linnhoff and Flower, 1978). The temperature, material concentration, and time act as quality parameters, whereas electricity, mass flowrate, and enthalpy are set as quantity parameters for the existing Pinch Analysis studies (Linnhoff and Hindmarsh, 1983). The versatile and flexibility of the Pinch Analysis to provide global targets for optimising the resources led to its application across various fields such as Total Site Heat (Klemeš et al., 1997), Water and Mass Analysis (Klemeš et al., 2014) and updated with the recent developments (Klemeš et al., 2018a), Water Pinch Analysis (Skouteris et al., 2018), Water Scarcity Pinch Analysis (Jia et al., 2020), Carbon Emission Pinch Analysis (Tan et al., 2018), Electric System Cascade Analysis (Ho et al., 2014a,b), Power Pinch Analysis (Liu et al., 2016), and Stand-alone Hybrid Power Pinch Analysis (Ho et al., 2014a,b). Jia et al. (2020) targeted all the water supply and demand streams in the Water Scarcity Pinch Analysis based on the water quality parameters, and recently Chin et al. (2021) extended Pinch Analysis to target and synthesise water recycling networks with multiple contaminants. A comprehensive review was presented by (Klemeš et al., 2018b) and the very recent second updated edition of the PI Handbook (Klemeš, 2022).

The water quality cascade was performed by classifying the water quality into different categories and then mixing and matching the water supplies and demands via downward compatibility rules. The work of water quality upgrading via water dilution method to maximise the water utilisation efficiency successfully maximise the utilisation of water. The Supply and Demand Composite Curves were introduced in the Pinch Analysis to maximise the utilisation of local resources. Alwi and Manan (2007) implemented the source and sink Composite Curves to reduce the freshwater demands by maximising water regeneration and free externally outsourced water. The graph of contaminant concentration versus mass flowrate was plotted during the mix and match of supply and demand curves. From the study, the water flowrate for utilities that required higher water purity was minimised. Skouteris et al. (2018) developed an analytic tool to manage water usage in the brick manufacturing industry. The water targeting strategy applied the Material Recovery Pinch Diagram (impurity versus flowrate graphical representation comprising supply and demand Composite Curves) to determine different water allocations for various processes.

## 2. Methodology

This section describes the methodology for mass flowrate allocation among the supply and demand streams. Since the focus of this work is to satisfy the C/N ratio required by the bioprocesses such as hydrogen (D1), methane (D2) and ethanol (D3) production, the mass flowrate of the resources in this analysis will only consider carbon and nitrogen components. Despite that, the rest of the organic components still account for the total mass flowrate while designing digester and waste storage capacity in future work. The general flowchart of this methodology is shown in Fig. 1.

A structure that illustrates the organic resources allocation is shown in Fig. 2, where the organic waste locally available (OWLA) are dairy manure (S1–C/N 13.4), swine manure (S2–C/N 15.8), kitchen waste (S3–C/N 20.3), rice straw (S4–C/N 44.1) and corn stover (S5–C/N 54.0). The organic waste from an external supply such as chicken manure (ES1-C/N 10.6), vinegar waste (ES2-C/N 22.9) and rice husk (ES3-C/N 103.5) would be required when the OWLA was not able to satisfy the demand sides for each of the case studies (Li et al., 2013). The bioprocesses such as hydrogen (D1), methane (D2) and ethanol (D3) production act as resource demand sides. Since the C/N ratio for each of the supply and demand sides varied across different online literature sources, therefore the C/N ratio might be an average value obtained from a few online literature references as references. Each of the organic waste and bioprocesses and their respective C/N ratio, together with the online references, were tabulated in Table 1. Pinch Analysis is a targeting tool and is often used as the initial step in determining the feasibility of a project. Detailed design in achieving the identified targets has to be carried out after targeting. In this study, the C/N ratio of the organic waste is the main consideration during the Pinch Analysis. The C/N ratio of the organic waste can be adapted accordingly based on the changes in composition, in terms of the C/N ratio, in different places. Three hypothetical case studies were created to illustrate different scenarios by varying the availability of OWLA, and the resources demand required.

Section 2.1 describes the organic waste resource allocation, such as the direct mass flowrate targeting, SCC end-shifting, SCC down-shifting, SCC right-shifting, and SCC detaching. Section 2.2 shows the application of each organic waste resource allocation in different scenarios. The goal is to maximise the utilisation of organic waste locally available (OWLA) while satisfying all the demand streams so that transportation activities of the resources are to be minimised. Transportation of the resources not only reduces the profit but also increases the carbon footprint of the bioprocesses. However, the cost and carbon emissions footprints are not discussed in this study since the focus of this study was to deal with the C/N ratio of the supply and demand sides. If OWLA was unable to satisfy the designated demands, external supply would be required. In this study, the ES is defined as the organic waste found outside of the studied area, denoted as external supply, ES.

### 2.1. *Construct mass flowrate table and plot C/N ratio Pinch Analysis Graph*

The resources mix and match and allocation for supply and demand streams were done via the C/N ratio SCC shifting techniques. The C/N ratio Pinch Analysis Graph plots cumulative carbon mass flowrate versus cumulative nitrogen mass flowrate. In this graph, the line's gradient represents the C/N ratio of the stream. A mass flowrate table was constructed before the C/N ratio Pinch Analysis graph was plotted. The construction of the Mass Flowrate Table is illustrated in Table 2, and the procedures were as follows:

Step 1 The supply/demand streams were organised in ascending order based on the corresponding C/N ratio number, C/N ratio. The stream and corresponding C/N ratio were arranged in Columns 1 and 2.

Step 2 The mass flowrate of each supply/demand stream, $MF_i$ (t/d), was arranged in Column 3. The mass flowrates of the organic waste only considered carbon (C) and nitrogen (N) elements instead of all organic elements. The individual mass flowrate for carbon, $MC_i$ (t/d) and nitrogen, $MN_i$ (t/d) was calculated via Eq (1) and Eq (2) and then arranged in Columns 4 and 5.

$$MC_i = \frac{N_{C/N}}{N_{C/N} + 1} \times MF_i \tag{1}$$

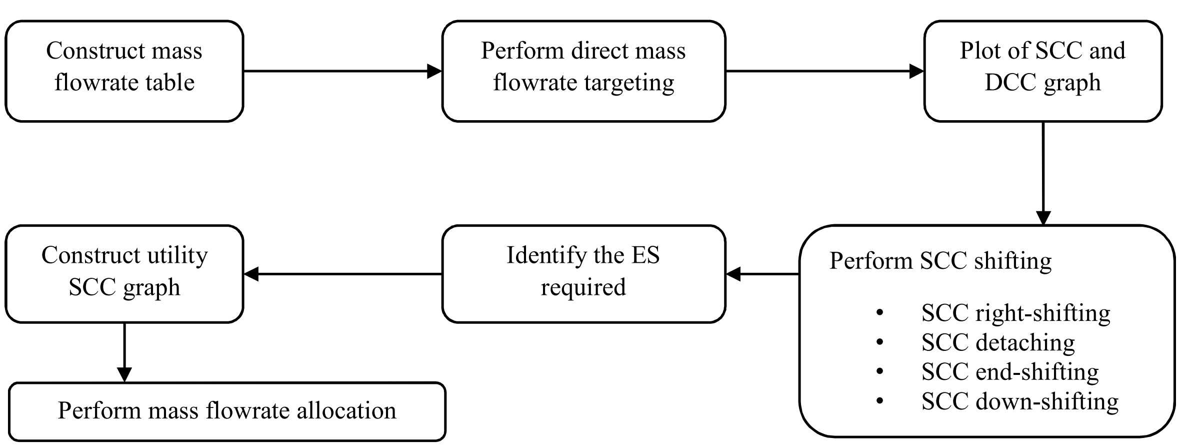


**Fig. 1.** Flow diagram of resources allocation in terms of C/N ratio.

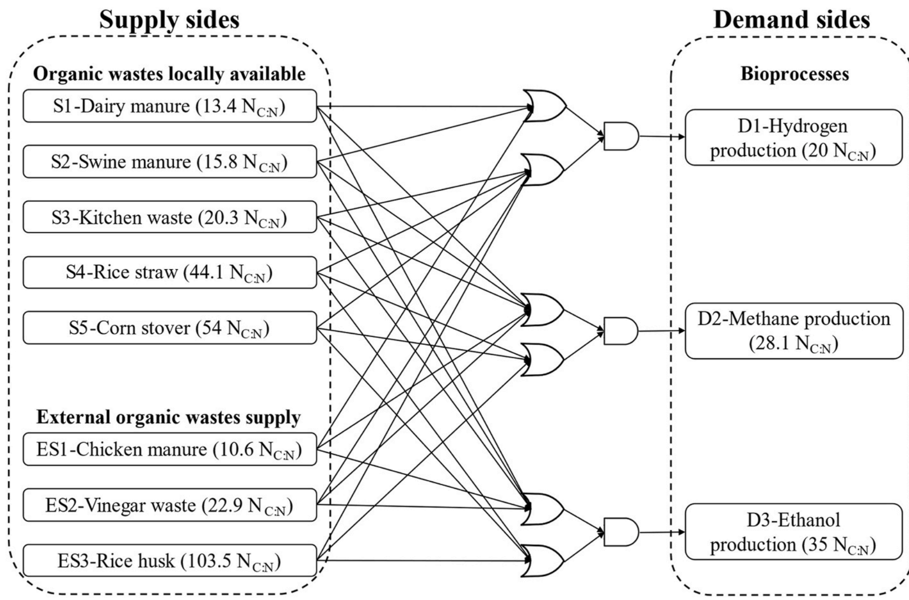


**Fig. 2.** Structure of supply and demand streams resource allocation.

**Table 1**
The C/N ratio required by each bioprocess.

| Bioprocess (Demand side) | C/N ratio required | Reference |
|---|---|---|
| Hydrogen | 15.01–23.01 | (Z. Li et al., 2018) |
| | 16–27 | Rawoof et al. (2021) |
| | Average = 20 | |
| Methane | 30 | Tanimu et al. (2014) |
| | 30.9 | Yong et al. (2015) |
| | 20 | Zhong et al. (2013) |
| | 25–30 | Wang et al. (2012) |
| | 45 | Beniche et al. (2020) |
| | 15.8 | Zhang et al. (2013) |
| | Average = 28.1 | |
| Ethanol | 35.2 | Manikandan and Viruthagiri (2010) |

**Table 2**
A sample mass flowrate table for demand streams.

| Demand Stream | C/N ratio | MF (t/d) | MC (t/d) | MN (t/d) | CMC (t/d) | CMN (t/d) |
|---|---|---|---|---|---|---|
| | | | | | 0 | 0 |
| D1 | 5 | 10 | 8.333 | 1.667 | 8.33 | 1.667 |
| D2 | 10 | 20 | 18.182 | 1.818 | 26.52 | 3.485 |
| D3 | 15 | 30 | 28.125 | 1.875 | 54.64 | 5.360 |

$$MN_i = \frac{1}{N_{C/N}+1} \times MF_i \tag{2}$$

Step 3 The cumulative MC, $CMC_i$ (t/d) against cumulative MN, $CMN_i$ (t/d) for supply and demand sides were calculated via Eq (3) and Eq (4). The $CMC_i$ and $CMN_i$ were arranged in Columns 6 and 7.

$$CMC_i = CMC_{i-1} + MC_i \tag{3}$$

$$CMN_i = CMN_{i-1} + MN_i \tag{4}$$

Step 4 The Supply and Demand Composite Curves (SCC and DCC) in the C/N ratio Pinch Analysis Graph were constructed by plotting the calculated $CMC_i$ against $CMN_i$.

## 2.2. Organic waste resource allocation

### 2.2.1. The direct mass flowrate targeting

The resource distribution should prioritise the utilisation of supply streams having the same C/N ratio as required by the demand stream. The direct mass flowrate targeting approach is executed when the C/N ratio required by demand streams is the same as the C/N ratio provided by the supply stream.

If the mass flowrate of the supply stream is more than the demand stream, the mass flowrate of the satisfied demand stream is denoted as 0. In that case, the surplus of supply streams, $MF_{surplusS}$, is calculated via Eq (5), where $MF_S$ is the mass flowrate of the supply stream, and $MF_D$ is the mass flowrate of the demand stream. On the other hand, if the mass flowrate of the supply stream is less than the demand stream, the supply stream's mass flowrate is denoted as 0, and the deficit mass flowrate of demand streams, $MF_{deficitD}$, is calculated by Eq (6).

$$MF_{surplusS} = MF_S - MF_D \tag{5}$$

$$MF_{deficitD} = MF_D - MF_S \tag{6}$$

An illustrated example was shown in Table 3 since the supply streams S2, and S4 have the same C/N ratio required by demand streams D2 and D3, and for this reason, the S2 and S4 mass flowrate distribution were prioritised to satisfy D2 and D3 separately. The graph of SCC and DCC before and after deduction is illustrated in Fig. 3. Please keep in mind that the C/N ratio used in this example does not reflect the actual C/N ratio; the data was created exclusively to illustrate when the supply and demand sides share the same C/N ratio. The SCC and DCC, after performing a direct mass flowrate targeting approach, continued with specific resource allocations in the next sub-section.

**Table 3**
Sample deduction of mass flowrates for supply and demand sides.

| Supply stream | C/N ratio | MF deduction (t/d) | | Demand stream | C/N ratio | MF deduction (t/d) | |
|---|---|---|---|---|---|---|---|
| | | Before | After | | | Before | After |
| S1 | 35 | 20 | 20 | D1 | 25 | 35 | 35 |
| S2 | 45 | 30 | 0 | D2 | 45 | 35 | 5 |
| S3 | 50 | 30 | 30 | D3 | 65 | 40 | 5 |
| S4 | 65 | 35 | 0 | | | | |

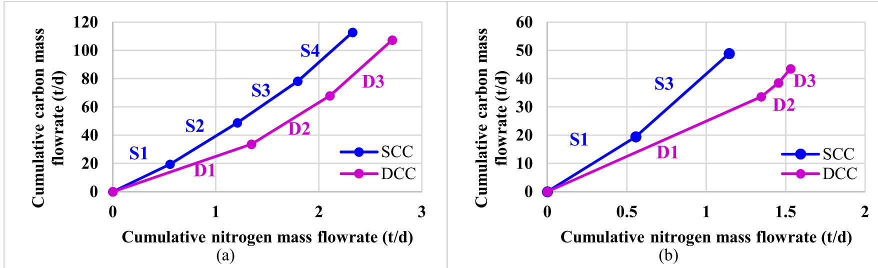


**Fig. 3.** Plot of the SCC and DCC (a) before and (b) after direct mass flowrate targeting.

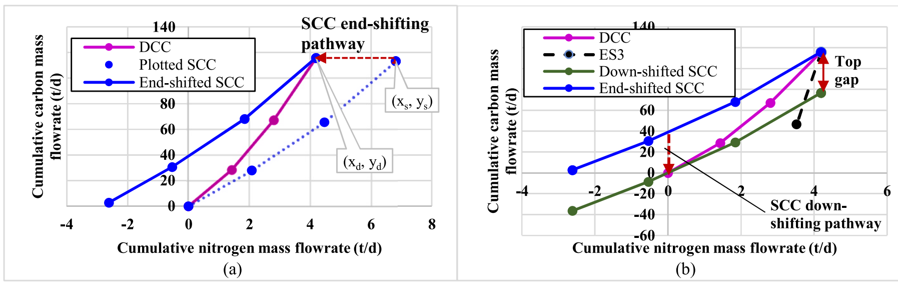


**Fig. 4.** The demonstration of (a) SCC end-shifting and (b) SCC down-shifting.

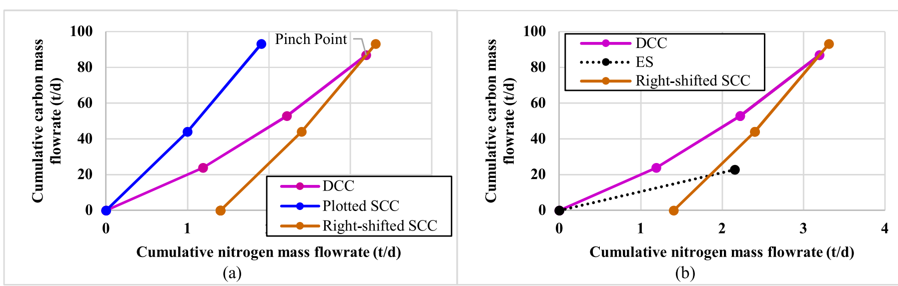


**Fig. 5.** The demonstration of the SCC right-shifting.

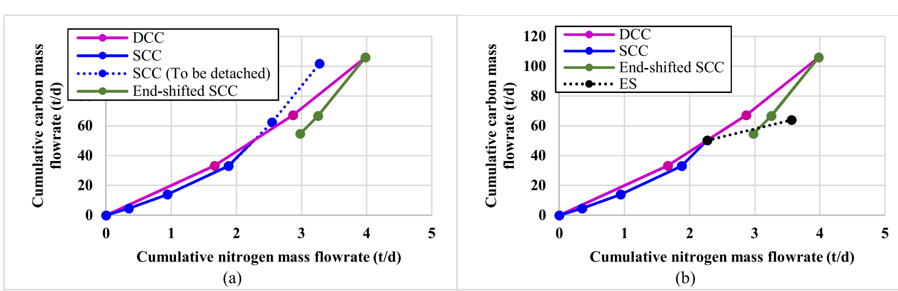


**Fig. 6.** The demonstration of (a) to-be detached SCC and (b) end-shifted SCC.

#### 2.2.2. *SCC end-shifting, SCC down-shifting, SCC right-shifting and SCC detaching*

There are four steps being introduced in this study while performing the organic waste resource allocation to satisfy the demand streams for each case study, namely SCC end-shifting, SCC down-shifting, SCC right shifting and SCC detaching. Each was executed based on the condition of the plotted SCC and DCC as follows.

Step 1 The SCC end-shifting approach was executed if the scenario with plotted SCC is located at the right of DCC, and at the same time, the SCC has an excessive supply of nitrogen (Fig. 4a).

Step 2 The SCC down-shifting was performed when the entire end-shifted SCC located t the left of DCC with the ending point of the end-shifted SCC met with the DCC (Fig. 4b). The external supply line was then drawn from the ending point of SCC against the x- and y-axes with the corresponding C/N ratio as a line gradient. The x- and y-axes lengths were plotted according to the mass flowrate of nitrogen and carbon available.

Step 3 For a scenario with plotted SCC located at the left of DCC, and at the same time the SCC has an insufficient supply of nitrogen, the SCC right-shifting approach will be executed (Fig. 5). The external supply line was plotted from the starting point of SCC based on the corresponding C/N ratio as the gradient. The x- and y-axes length was plotted according to the mass flowrate of nitrogen and carbon available.

Step 4 For the scenario with plotted SCC partially located at the right of DCC, and at the same time, part of the plotted SCC located on the left of DCC was required to be detached (Fig. 6a) and perform the SCC end-shifting approach (Fig. 6b).

### 2.3. Case studies

Three biodigesters were required to fulfil the biomethane, biohydrogen and bioethanol demands by valorising the organic waste available within a town. Each organic waste was assumed to have a stable mass flowrate every day. Each biodigester focus on one main product that is biomethane, biohydrogen and bioethanol. This study aimed to target the demand streams by allocating the mass flowrate of organic waste locally available (OWLA) to each biodigester. The OWLA in this study is an illustrative organic waste with their C/N ratio found within the studied area. The mass flowrate of supply and demand streams for each case study were listed in Table 4 and Table 5. Specific SCC shifting was developed for each case study while targeting demand streams and allocating the mass flowrate of supply streams. The organic waste supply from an external supply (ES) was required when the OWLA could not satisfy the demand side. In this study, three ES was defined as organic waste available outside the studied town, namely chicken manure (ES1), vinegar waste (ES2) and rice husk (ES3) (Table 6). If multiple streams of ES are eligible to satisfy the requirement, lesser stream number and lower mass flowrate required are preferable as they minimise the frequency of transportation of external supply. The ES was set as a backup supply to mix with OWLA to satisfy the demand streams.

#### 2.3.1. Case study 1

For Case Study 1, there are three designated bioprocesses demands (Table 4), namely hydrogen (D1), methane (D2) and ethanol (D3), required to be satisfied by valorising the OWLA found in Case Study 1, namely dairy manure (S1), swine manure (S2) and kitchen waste (S3) (Table 5). A mass flowrate table was constructed before plotting the C/N ratio Pinch Analysis graph.

*2.3.1.1. Construct mass flowrate table and plot C/N ratio Pinch Analysis graph.* The steps (1) to step (4) in Section 2.1 were applied to construct the mass flowrate table for Case Study 1 (Table 7 and Table 8) and tabulated in Fig. 7.

*2.3.1.2. Perform SCC end-shifting followed by down-shifting.* Based on the mass flowrate and C/N ratio of the Resource Supply and Demand Side, the plotted SCC was located at the right of DCC, and the total nitrogen cumulative mass flowrate of plotted SCC was greater than DCC. The entire plotted SCC was shifted until the ending point of shifted SCC and DCC overlapped on the same point. This approach prioritises the mass flowrate utilisation of OWLA resources with a higher C/N ratio to maximise the utilisation of OWLA. The steps to perform SCC end-shifting approach to determine the ES required were as follows:

Step 1 The x- and y-axis distances between the ending points for SCC and DCC, denoted as $D_x$ and $D_y$, were calculated via Eq (5) and Eq (6), where the coordinates ($x_s$, $y_s$) and ($x_d$, $y_d$) were the ending points for SCC and DCC.

$$D_x = (x_d - x_s) \quad (5a)$$

**Table 4**
The different mass flowrate of demand streams for three case studies.

| Supply stream | Bioprocesses | C/N ratio | Mass flowrate (t/d) | | |
|---|---|---|---|---|---|
| | | | Case Study 1 | Case Study 2 | Case Study 3 |
| D1 | Hydrogen | 20 | 30 | 25 | 35 |
| D2 | Methane | 28.1 | 40 | 30 | 35 |
| D3 | Ethanol | 35 | 50 | 35 | 40 |

**Table 5**
The different mass flowrate of supply streams for three case studies.

| Supply stream | Organic waste | C/N ratio | Mass flowrate (t/d) | | |
|---|---|---|---|---|---|
| | | | Case Study 1 | Case Study 2 | Case Study 3 |
| S1 | Dairy manure | 13.4 | 30 | 0 | 5 |
| S2 | Swine manure | 15.8 | 40 | 0 | 10 |
| S3 | Kitchen waste | 20.3 | 50 | 0 | 20 |
| S4 | Rice straw | 44.1 | 0 | 45 | 30 |
| S5 | Corn stover | 54.0 | 0 | 50 | 40 |

**Table 6**
Organic waste from an ES and its corresponding C/N ratio (Y. Li et al., 2013).

| External supply stream | Organic waste | C/N ratio |
|---|---|---|
| ES 1 | Chicken manure | 10.6 |
| ES 2 | Vinegar waste | 22.9 |
| ES 3 | Rice husk | 103.5 |

**Table 7**
The mass flowrates of OWLA in Case Study 1.

| Supply stream (OWLA) | C/N ratio | MF (t/d) | MC (t/d) | MN (t/d) | CMC (t/d) | CMN (t/d) |
|---|---|---|---|---|---|---|
| S1 (Dairy manure) | 13.4 | 30 | 27.917 | 2.083 | 27.92 | 2.083 |
| S2 (Swine manure) | 15.8 | 40 | 37.619 | 2.381 | 65.54 | 4.464 |
| S3 (Kitchen waste) | 20.3 | 50 | 47.653 | 2.347 | 113.19 | 6.812 |

**Table 8**
The mass flowrates of demand streams in Case Study 1.

| Demand stream | C/N ratio | MF (t/d) | MC (t/d) | MN (t/d) | CMC (t/d) | CMN (t/d) |
|---|---|---|---|---|---|---|
| | | | | | 0 | 0 |
| D1 (Hydrogen) | 20 | 30 | 28.571 | 1.429 | 28.57 | 1.429 |
| D2 (Methane) | 28.1 | 40 | 38.625 | 1.375 | 67.20 | 2.803 |
| D3 (Ethanol) | 35 | 50 | 48.611 | 1.389 | 115.81 | 4.192 |

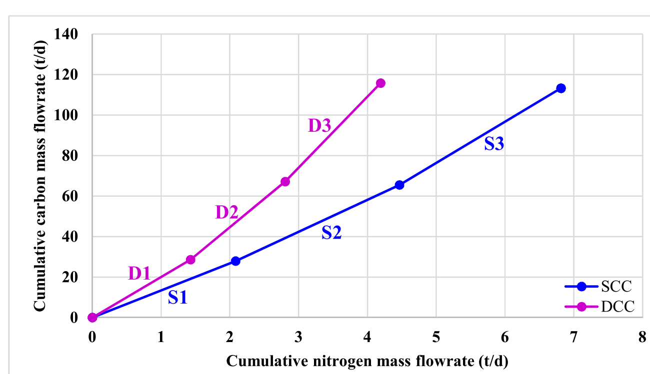


**Fig. 7.** The SCC and DCC for case study 1.

$$D_y = (y_d - y_s) \tag{6a}$$

Step 2 The entire SCC shift along the x- and y-axes if the values of $D_x$ and $D_y$ are positive and vice versa.
Step 3 Part of the end-shifted SCC located above the DCC was identified as an SCC section to be detached.

The plotted SCC was shifted 3.538 and 1.462 t/d against the x- and y-axes based on the calculated $D_x$ and $D_y$ value of −3.538, −1.462 (Fig. 8). Since the SCC has to be located at the right of DCC to satisfy the demand streams, SCC down-shifting was performed on the end-shifted SCC.

*2.3.1.3. Perform SCC down-shifting.* The steps to perform SCC end-shifting approach were as follows:

Step 1 The y-intercept constant of the particular to-be down-shifted SCC line equation (y = 15.8x+39.011) crossing the y-axis origin was denoted as $D_{y0}$.
Step 2 The to-be down-shifted SCC was then shifted against the y-axis according to the value of the SCC down-shifting pathway, $D_{y0}$, resulting in the down-shifted SCC intercepted with the origin of the graph (Fig. 9).

The y-intercept of the end-shifted SCC (line S2) crossed the y-axis was identified as 39.011. The entire end-shifted SCC was shifted 39.011 t/d against the y-axis until the down-shifted SCC crossed the graph's origin (Fig. 9). Since the down-shifted SCC could not form a closed-loop at the ending point of DCC, extra resource supply was required to satisfy the demand streams. If the top gap was formed, an ES line would be plotted from the ending point of the DCC ($x_d$, $y_d$) against the x- and y-axes until it intercepts with the down-shifted SCC at an interception point ($x_i$, $y_i$) and forms a closed-loop.

*2.3.1.4. Determine valid and preferred external supply.* Case study 1 was tested with three illustrated ES with a C/N ratio of 10.6, 22.9 and 103.5 to determine the valid and most suitable ES. The steps to determine the valid and preferred ES were as follows:

Step 1 An ES line was plotted according to the C/N ratio as a line gradient from the ending point of the DCC ($x_d$, $y_d$) along the x- and y-axes until it intercepted with the down-shifted SCC at an interception point ($x_i$, $y_i$) and formed a closed-loop (Fig. 10).
Step 2 Part of the down-shifted SCC formed a closed-loop with the ES was identified as the utility OWLA. At the same time, part of the down-shifted SCC did not involve forming the closed-loop identified as OWLA in excess and was discharged.

Despite there being three ES available, only ES3 was valid because

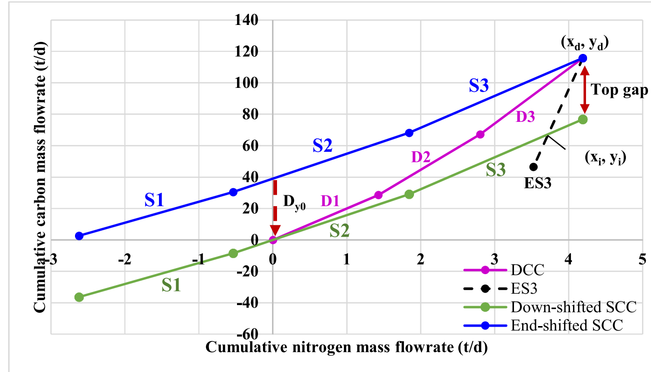


**Fig. 9.** The end-shifted and down-shifted SCC for Case Study 1.

the C/N ratio of the ES has to be greater than or equal to the C/N ratio of the demand stream (D3) closest to the top gap and only line ES3 was eligible to form a closed-loop with the OWLA. The plotted ES3 line was intercepted with the down-shifted SCC (line S3) at the coordinate of (3.723, 67.279), as reflected in Fig. 10.

*2.3.1.5. Construct utility SCC comprised of utility OWLA and selected external supply.* The interception point formed between line ES 3 and line S3 act as a reference point to determine the mass flowrates of the utility OWLA, excess OWLA, and ES required. Part of the down-shifted SCC from the origin to the interception point represents the mass flowrate of the OWLA that will be utilised to satisfy the demand stream, denoted as utility OWLA. In addition, the portion of SCC not involved in forming the closed-loop between SCC and DCC was identified as the OWLA in excess and will be discharged, denoted as excess OWLA. Also, the mass flowrate of ES 3 required to satisfy Case Study 1 was identified from the ending point of DCC until the interception point. The total mass flowrates of the ES, $MF_{ES}$ (t/d) were calculated via Eq (7), where ($x_a$, $y_a$) and ($x_i$, $y_i$) are the starting and ending point of the line ES.

$$MF_{ES} = |(y_a - y_i) + (x_a - x_i)| \tag{7}$$

From the calculations, the total mass flowrates required by ES 3 to satisfy the demand streams was 48.998 t/d, as described in Table 9. Part of the down-shifted SCC section forming a closed-loop from (0, 0) to (1.845, 29.144) and from (1.845, 29.144) to (3.7232, 67.2793) was identified as the utility OWLA. The mass flowrate of each supply stream utilised to satisfy the demand streams and unutilised was calculated via Eq (7) and presented in Table 10. The MC, MN, CMC and CMN for the utility supply streams comprised utility OWLA and ES 3 were calculated via Eq (1) to Eq (4) and listed in Table 11. A utility SCC graph was plotted using the utility supply stream for Case Study 1 in Fig. 11.

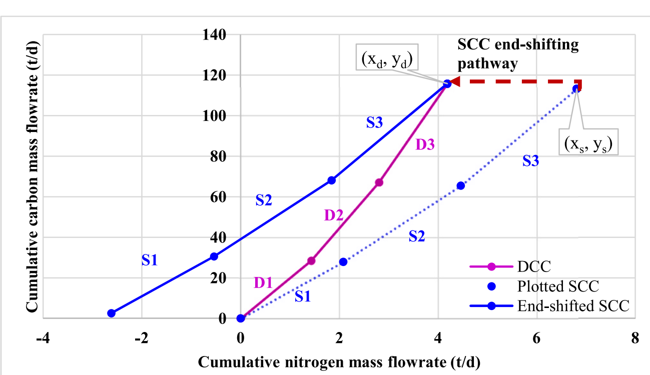


**Fig. 8.** The plotted SCC and the end-shifted SCC for Case Study 1.

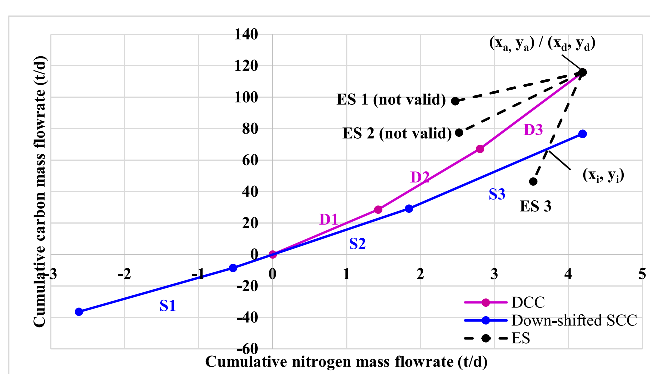


**Fig. 10.** Determination of eligible and preferred ES for Case Study 1.

**Table 9**
The mass flowrate of different ES tested for Case Study 1.

| External supply | C/N ratio | Starting point ($x_a$, $y_a$) | Ending point ($x_i$, $y_i$) | MF (t/d) | MC (t/d) | MN (t/d) |
|---|---|---|---|---|---|---|
| ES1 (Chicken manure) | 10.6 | (4.192, 115.808) | – | – | – | – |
| ES2 (Vinegar waste) | 22.9 | (4.192, 115.808) | – | – | – | – |
| ES3 (Rice husk) | 103.5 | (4.192, 115.808) | (3.7232, 67.279) | 48.998 | 48.529 | 0.469 |

**Table 10**
The mass flowrate status of OWLA and ES supply streams for Case Study 1.

| Supply streams | C/N ratio | Mass flowrate (t/d) | | |
|---|---|---|---|---|
| | | Available (t/d) | Utilised (t/d) | Not utilised (t/d) |
| S1 (Dairy manure) | 13.4 | 30 | – | 30 |
| S2 (Swine manure) | 15.8 | 40 | 30.989 | 9.011 |
| S3 (Kitchen waste) | 20.3 | 50 | 40.013 | 9.987 |
| ES3 | 103.5 | N/A | 48.998 | N/A |

**Table 11**
The mass flowrates of utility supply streams for Case Study 1.

| Utility supply stream | C/N ratio | MF (t/d) | MC (t/d) | MN (t/d) | CMC (t/d) | CMN (t/d) |
|---|---|---|---|---|---|---|
| | | | | | 0 | 0 |
| S2 (Swine manure) | 15.8 | 30.989 | 29.144 | 1.845 | 29.144 | 1.845 |
| S3 (Kitchen waste) | 20.3 | 40.013 | 38.135 | 1.879 | 67.279 | 3.723 |
| ES3 (Rice husk) | 103.5 | 48.529 | 48.529 | 0.469 | 115.808 | 4.192 |

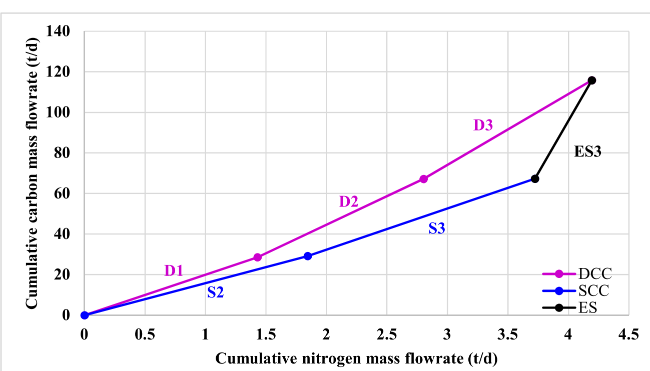


**Fig. 11.** The utility SCC comprised utility OWLA and ES3 for Case Study 1.

*2.3.1.6. Utility supply streams mass flowrate allocation.* The utility supply streams mass flowrate allocation starts from the demand stream D1, which requires the lowest C/N ratio requirement among the demand streams (Fig. 12a). Utility supply stream mixing was required during targeting demand stream D1 because no closed-loop was formed to enclose the starting and ending point of targeted demand stream D1. So, the supply stream ES3 with the highest C/N ratio among the utility supply streams was required to shift until the ending point of line ES3 met with the ending point of line D1.

The $D_x$ and $D_y$ between the line ES3 and D1's ending points were calculated as −2.763 and −87.237 t/d via Eq (5) and Eq (6). Thus, the line ES3 was shifted 2.763 and 87.237 t/d against the x- and y-axes. The shifted line ES3 intercepted with line S2 and formed a closed-loop indicating that line D1 was satisfied.

Part of the utility SCC from the starting point of line D1 to the interception point (1.360, 21.491) and part of the shifted line ES3 from the interception point to the ending point of line D1 were identified as mass flowrate used to satisfy the targeted demand stream D1. The carbon and nitrogen mass flowrates ($MCU_i$ and $MNU_i$) of each supply stream utilised to satisfy the targeted demand steam were calculated via Eq (8) and Eq (9), where ($x_2$, $y_2$) and ($x_1$, $y_1$) represent the ending and starting point of each utilised supply stream.

$$MCU_i = (y_2 - y_1) \tag{8}$$

$$MNU_i = (x_2 - x_1) \tag{9}$$

The shifted line ES3 below the interception point and the utility SCC above the interception point were then identified as unutilised utility resources. The unutilised utility resources formed a new utility SCC at the subsequent unsatisfied demand stream's starting point with the lowest C/N ratio requirement (Fig. 12b). Similar mass flowrate allocation steps in targeting demand stream D1 were replicated to satisfy the rest of the demand streams, as demonstrated in (Fig. 12c) and (Fig. 12d). The mass flowrate allocations for Case Study 1 were summarised and tabulated in Table 12.

### 2.3.2. Case study 2

For Case Study 2, there are two types of OWLA (Table 13), namely rice straw (S4) and corn stover (S5), that can be valorised to meet the designated bioprocesses demands (Table 14). The SCC and DCC for Case Study 2 were plotted as in Fig. 13 using the calculated CMC and CMN for the supply and demand sides.

*2.3.2.1. Perform SCC right-shifting.* Based on the mass flowrate and C/N ratio of the resource supply and demand side for Case Study 2, the plotted SCC was located at the left of DCC, and the total nitrogen cumulative mass flowrate of plotted SCC was lesser than DCC. The entire plotted SCC was shifted to the right until the entire SCC was located at the right of DCC, with the formation of a Pinch Point. As illustrated in Fig. 14, the plotted SCC was shifted 1.403 t/d along the x-axis, forming a Pinch Point at the ending point of line D3 (3.194, 86.806). After the SCC right-shifting approach was performed, the formation of a bottom gap indicated the OWLA resources were unable to satisfy the demand streams completely, and the ES was required to import from the foreign regions to mix with the OWLA. The ES line was plotted according to the corresponding C/N ratio as a line gradient.

*2.3.2.2. Determine valid and preferred external supply.* Case Study 2 was tested with three illustrated ES with a C/N ratio of 10.6, 22.9 and 103.5 to determine the valid and most suitable ES. At the bottom gap, the ES that is eligible to mix with OWLA must have a C/N ratio smaller than demand stream D1 so that the closed-loop formed is located at the right of DCC. The steps to determine the eligible and preferred ES were as follows:

Step 1 If the bottom gap formed, an ES line was plotted from the starting point of the DCC ($x_d$, $y_d$) along the x- and y-axes until it intercepts with the right-shifted SCC at an interception point ($x_i$, $y_i$) and forms a closed-loop.

Step 2 If the top gap formed, an ES line was plotted from the ending point of the DCC ($x_d$, $y_d$) against the x- and y-axes until it intercepts with the right-shifted SCC at an interception point ($x_i$, $y_i$) and forms a closed-loop.

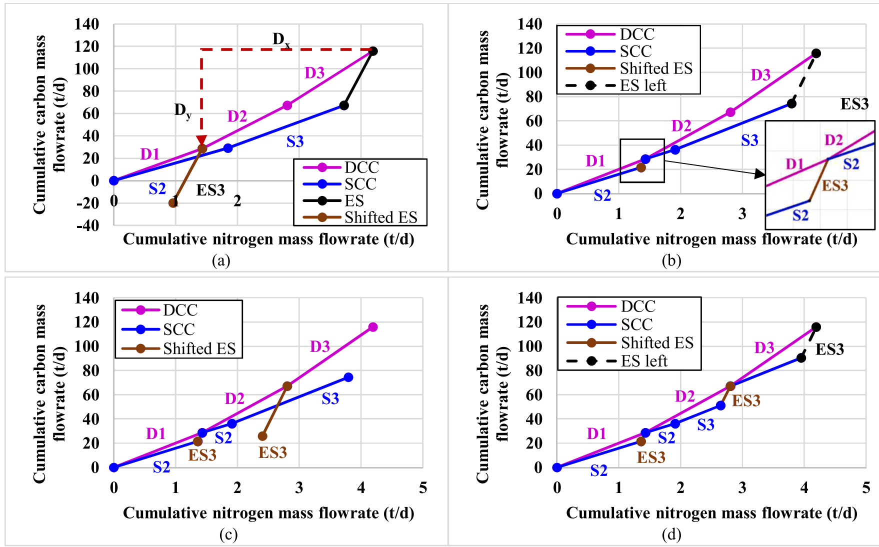


**Fig. 12.** Mass flowrate allocation of utility supply streams for (a and b) Demand 1 (c) Demand 2 (d) Demand 3 in Case Study 1.

**Table 12**
The mass flowrate allocation of utility supply streams for Case Study 1.

| Utility supply stream | Mass flowrate received (t/d) | | |
|---|---|---|---|
| | Demand Stream 1 | Demand Stream 2 | Demand Stream 3 |
| S2 (Swine manure) | 22.851 | 8.138 | – |
| S3 (Kitchen waste) | – | 15.659 | 24.355 |
| ES3 (Rice husk) | 7.149 | 16.204 | 25.645 |

**Table 13**
The mass flowrates table of OWLA in Case Study 2.

| Supply stream (OWLA) | C/N ratio | MF (t/d) | MC (t/d) | MN (t/d) | CMC (t/d) | CMN (t/d) |
|---|---|---|---|---|---|---|
| | | | | | 0 | 0 |
| S4 (Rice straw) | 44.1 | 45 | 44.002 | 0.998 | 44.002 | 0.998 |
| S5 (Corn stover) | 54.0 | 50 | 49.091 | 0.909 | 93.093 | 1.907 |

**Table 14**
The mass flowrates table of demand stream in Case Study 2.

| Demand stream | C/N ratio | MF (t/d) | MC (t/d) | MN (t/d) | CMC (t/d) | CMN (t/d) |
|---|---|---|---|---|---|---|
| | | | | | 0 | 0 |
| D1 (Hydrogen) | 20 | 25 | 23.810 | 1.190 | 23.810 | 1.190 |
| D2 (Methane) | 28.1 | 30 | 28.969 | 1.031 | 52.779 | 2.221 |
| D3 (Ethanol) | 35 | 35 | 34.028 | 0.972 | 86.806 | 3.194 |

Step 3 As the aim is to maximise the utilisation of OWLA, the ES with a C/N ratio as low as possible is preferable to fill the bottom gap. In contrast, an ES with a C/N ratio as high as possible is preferable to fill the top gap.

Among the three ES, only ES 1 was eligible to fill the bottom gap among the three ES available as ES 1's C/N ratio was smaller than the C/N ratio of demand stream D1. So, the line ES 1 was linked from the DCC's starting point along the x- and y-axes until intercepted with the right-shifted SCC. The plotted ES 1 line was intercepted with the right-shifted SCC (line S4) at the coordinate of (1.847, 19.580), as shown in Fig. 15.

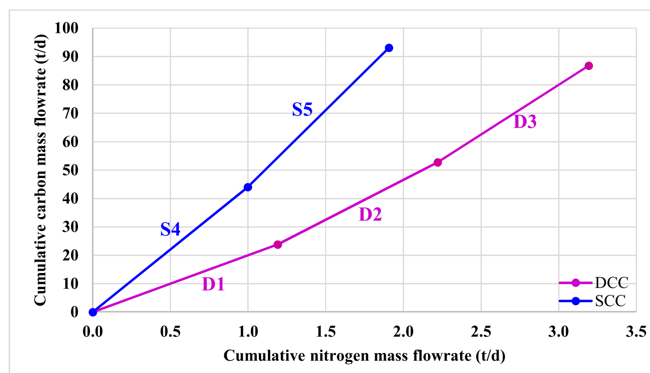


**Fig. 13.** The SCC and DCC for case study 2.

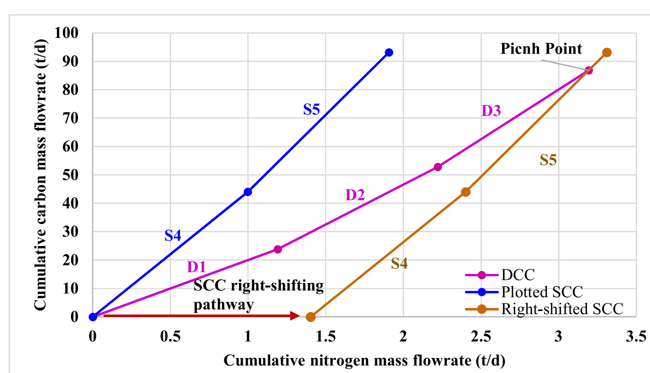


**Fig. 14.** The plotted SCC and right-shifted SCC for Case Study 2.

The interception point formed between line ES 1 and right-shifted line S4 acts as a reference point to determine the mass flowrates of the utility OWLA, excess OWLA and ES required. Part of the right-shifted SCC from the interception point to the Pinch Point represents the mass flowrate of the OWLA that will be utilised to satisfy the demand stream, denoted as utility OWLA. In addition, the part of SCC located below the interception point is the OWLA in excess and was discharged, denoted as excess OWLA. The mass flowrate of ES 1 was also required to satisfy the bottom gap of Case Study 2 was identified from the starting point of DCC

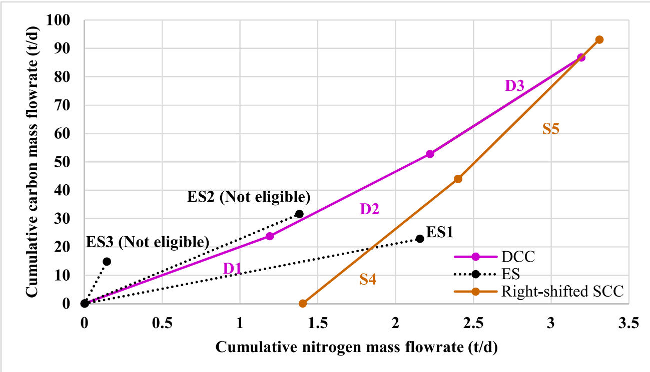


**Fig. 15.** Determine eligible and preferred ES for the bottom gap of Case Study 2.

until the interception point. The MF, MC and MN of ES 1 used to fill the bottom gap were calculated via Eq (7), Eq (1) and Eq (2), respectively (Table 15).

*2.3.2.3. Construct utility SCC comprised of utility OWLA and external supply 1.* The mass flowrate of each supply stream that will be utilised and discharged was calculated via Eq (7) and presented in Table 16. The MC, MN, CMC and CMN for the utility supply streams comprised utility OWLA and ES 1 were calculated via Eq (1) to Eq (4) and listed as per Table 17. Then, a utility SCC was plotted using the utility supply stream for Case Study 2 in Fig. 16.

*2.3.2.4. Utility supply streams mass flowrate allocation.* The utility supply streams mass flowrate allocation for Case Study 2 starts from the demand stream D1, with the lowest C/N ratio requirement among the demand streams. As the ending point of a line, D1 does not form a closed-loop with the plotted utility SCC; supply stream adjustment was required. The supply stream S5, with the highest C/N ratio among the utility supply streams available, was required to shift until the ending point of line S5 met with the ending point of line D1, as shown in Fig. 17.

The $D_x$ and $D_y$ between the ending points of line S5 and line D1 were calculated as −2.003 t/d and −62.997 t/d via Eq (5) and Eq (6). The line S5 was shifted 2.003 and 62.997 t/d against the x- and y-axes. The line ES1 intercepted with shifted line S5 formed a closed-loop indicating that line D1 was satisfied. Part of the utility SCC from starting point of line D1 to the interception point (0.933, 9.886) and part of the shifted line S5 from the interception point to the ending point of line D1 were identified as mass flowrate used to satisfy the targeted demand stream D1. The MCU and MNU of each utility supply stream in fulfilling the demand stream D1 were calculated via Eq (8) and Eq (9).

Then, the mass flowrates of shifted line S5 below the interception point and the utility SCC above the interception point were identified as unutilised utility resources. The unutilised utility resources formed a new SCC at the starting point of the subsequent unsatisfied demand stream with the lowest C/N ratio requirement. Similar mass flowrate allocation steps in targeting demand stream D1 were repeated to satisfy the rest of the demand streams (Fig. 18). The mass flowrate allocations for Case Study 2 were summarised and tabulated in Table 18.

**Table 15**
The mass flowrate of different ES tested for bottom gap of Case Study 2.

| External supply | C/N ratio | Starting point ($x_a$, $y_a$) | Ending point ($x_i$, $y_i$) | MF (t/d) | MC (t/d) | MN (t/d) |
|---|---|---|---|---|---|---|
| ES1 (Chicken manure) | 10.6 | (0, 0) | (1.847, 19.580) | 21.427 | 19.580 | 1.847 |
| ES2 (Vinegar waste) | 22.9 | (0, 0) | – | – | – | – |
| ES3 (Rice husk) | 103.5 | (0, 0) | – | – | – | – |

**Table 16**
The mass flowrate status of OWLA and ES supply streams for Case Study 2.

| Supply streams | C/N ratio | Mass flowrate (t/d) | | |
|---|---|---|---|---|
| | | Available (t/d) | Utilised (t/d) | Not utilised (t/d) |
| ES1 (Chicken manure) | 10.6 | N/A | 21.427 | N/A |
| S4 (Rice straw) | 44.1 | 45 | 24.422 | 20.578 |
| S5 (Corn stover) | 54 | 50 | 42.802 | 7.198 |

**Table 17**
The mass flowrates of utility supply streams for Case Study 2.

| Utility supply stream | C/N ratio | MF (t/d) | MC (t/d) | MN (t/d) | CMC (t/d) | CMN (t/d) |
|---|---|---|---|---|---|---|
| | | | | | 0 | 0 |
| ES1 (Chicken manure) | 10.6 | 21.427 | 19.580 | 1.847 | 19.580 | 1.847 |
| S4 (Rice straw) | 44.1 | 24.422 | 24.422 | 0.554 | 44.002 | 2.401 |
| S5 (Corn stover) | 54 | 42.802 | 42.802 | 0.793 | 86.804 | 3.194 |

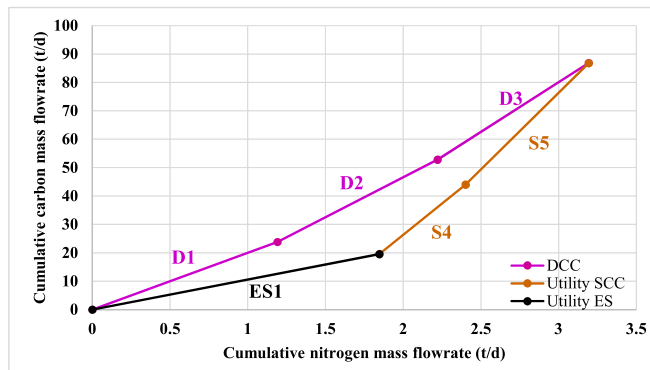


**Fig. 16.** The utility SCC comprised of utility OWLA, ES1 and ES3 for Case Study 2.

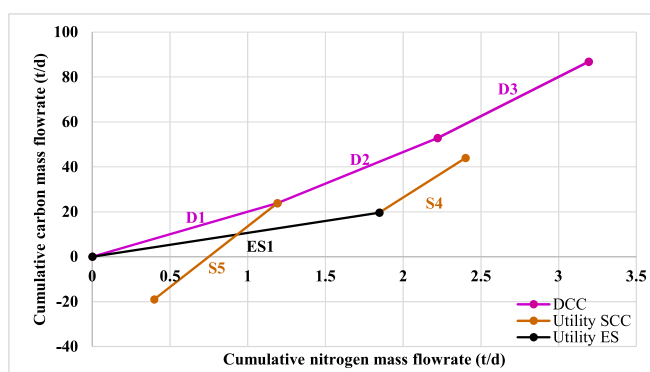


**Fig. 17.** Targeting of D1 by shifting the supply stream available with the highest CN ratio for Case Study 2.

### *2.3.3. Case study 3*

For Case Study 3, there are five types of OWLA (Table 19), namely

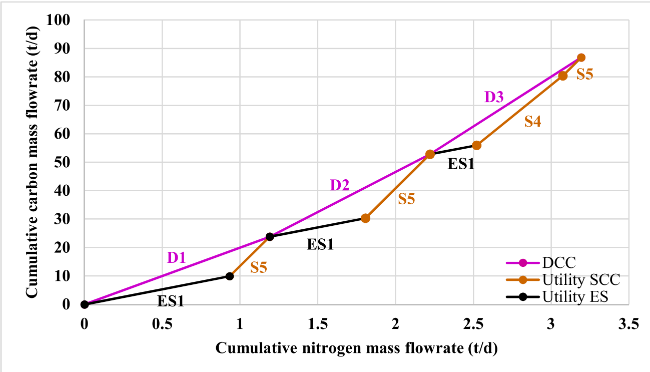


**Fig. 18.** Targeting the rest of the demand streams by shifting the supply stream available with the highest CN ratio for Case Study 2.

**Table 18**
The mass flowrate allocation of utility supply streams for Case Study 2.

| Utility supply stream | Mass flowrate received (t/d) | | |
|---|---|---|---|
| | Demand Stream 1 | Demand Stream 2 | Demand Stream 3 |
| ES1 (Chicken manure) | 10.819 | 7.136 | 3.473 |
| S4 (Rice straw) | – | – | 24.976 |
| S5 (Corn stover) | 14.182 | 22.864 | 6.549 |

**Table 19**
The mass flowrates for OWLA in Case Study 3.

| Supply stream (OWLA) | C/N ratio | MF (t/d) | MC (t/d) | MN (t/d) | CMC (t/d) | CMN (t/d) |
|---|---|---|---|---|---|---|
| | | | | | 0 | 0 |
| S1 (Dairy manure) | 13.4 | 5 | 4.653 | 0.347 | 4.653 | 0.347 |
| S2 (Swine manure) | 15.8 | 10 | 9.405 | 0.595 | 14.058 | 0.942 |
| S3 (Kitchen waste) | 20.3 | 20 | 19.061 | 0.939 | 33.119 | 1.881 |
| S4 (Rice straw) | 44.1 | 30 | 29.335 | 0.665 | 62.453 | 2.547 |
| S5 (Corn stover) | 54.0 | 40 | 39.273 | 0.727 | 101.726 | 3.274 |

dairy manure (S1), swine manure (S2) and kitchen waste (S3), rice straw (S4) and corn stover (S5), can be valorised to meet the designated bioprocesses demands (Table 20). The SCC and DCC for Case Study 3 were plotted as in Fig. 19 using the calculated CMC and CMN for the supply and demand sides.

*2.3.3.1. Perform SCC detaching.* Based on the mass flowrate and C/N ratio of the resource supply and demand side, the beginning part of the plotted SCC was on the right of DCC, and part of the SCC was on the left of DCC. Part of the DCC that formed a closed-loop with the plotted SCC indicated that particular part was satisfied. A gap at the ending point of DCC indicates that a particular part of the DCC was not satisfied, and ES

**Table 20**
The mass flowrates of demand streams in Case Study 3.

| Demand stream | C/N ratio | MF (t/d) | MC (t/d) | MN (t/d) | CMC (t/d) | CMN (t/d) |
|---|---|---|---|---|---|---|
| | | | | | 0 | 0 |
| D1 (Hydrogen) | 20 | 35 | 33.333 | 1.667 | 33.333 | 1.667 |
| D2 (Methane) | 28.1 | 35 | 33.797 | 1.203 | 67.131 | 2.869 |
| D3 (Ethanol) | 35 | 40 | 38.889 | 1.111 | 106.019 | 3.981 |

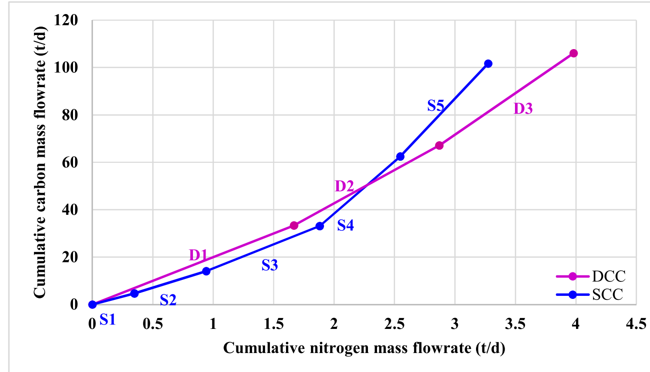


**Fig. 19.** The SCC and DCC for case study 3.

has to mix with the OWLA to fulfil the demand steams in Case Study 3. According to the existing Water Pinch Analysis, the closed-loop has to be formed at the right of DCC, part of the SCC located at the left of DCC was identified, and SCC-end shifting was performed. The plotted SCC located on the left of the DCC from (2.272, 50.343) to (2.547, 62.453) and from (2.547, 62.453) to (3.274, 101.726) were detached and shifted 0.707 and 4.293 t/d along the x- and y-axes based on the $D_x$ and $D_y$ value calculated via Eq (5) and Eq (6) (Fig. 20). After the SCC right-shifting approach was performed on the detached SCC, the formation of the gap between the starting point of the end-shifted SCC and the detaching point indicates the DCC was not satisfied, and the ES was required to mix with the OWLA in order to satisfy the DCC. The ES line was plotted according to the corresponding C/N ratio as a line gradient.

*2.3.3.2. Determine valid and preferred external supply.* Case study 3 was tested with three ES with a C/N ratio of 10.6, 22.9 and 103.5 to identify which ES is suitable and able to utilise more OWLA while satisfying the demand streams. At the gap, since the ES line will be plotted from the detaching point within the line D2, thus the ES that is eligible to mix with OWLA must have a C/N ratio lesser than or equal to the C/N ratio of line D2, which was 28.1. Among the three ESs, only ES 1 and ES 2 were eligible to satisfy the demand stream and formed a closed-loop at the right of DCC (Fig. 21). ES 1 having a smaller C/N ratio compared to ES 2 was preferable as it could maximise the utilisation of OWLA. The ES 1 linked from the detaching point along the x- and y-axes until it intercepted with the end-shifted SCC at (3.074, 58.845).

The interception point formed between line ES 1 and end-shifted line S4 acts as a reference point to determine the mass flowrates of the utility OWLA, excess OWLA and ES required. Part of the end-shifted SCC from the ending point of DCC to the interception point represents the mass flowrate of the OWLA that will be utilised to satisfy the demand stream,

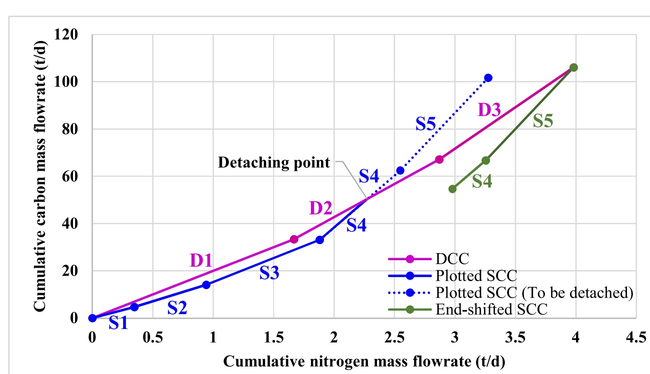


**Fig. 20.** The plotted SCC, to-be detached SCC and end-shifted SCC for Case Study 3.

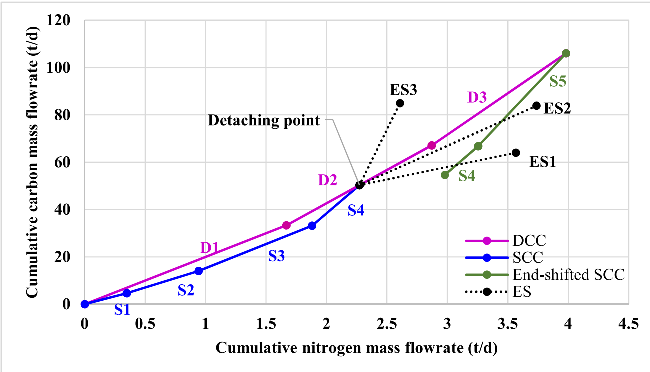


**Fig. 21.** Determine eligible and preferred ES for a top gap of Case Study 3.

denoted as utility OWLA. In addition, the part of end-shifted SCC located below the interception point is the OWLA in excess and will be discharged, denoted as excess OWLA. Also, the mass flowrate of ES 1 required to satisfy Case Study 3 was identified from the Pinch Point until the interception point. The MF, MC and MN of ES 1 and ES 2 that were validated to be used to fill the top gap were calculated via Eq (7), Eq (1) and Eq (2), respectively (Table 21).

*2.3.3.3. Construct utility SCC comprised of utility OWLA and external supply 1.* The mass flowrate of each supply stream that will be utilised and discharged was calculated via Eq (7) and presented in Table 22. The MC, MN, CMC and CMN for the utility supply streams comprised utility OWLA and ES 1 were calculated via Eq (1) to Eq (4) and listed as per Table 23. Then, a utility SCC was plotted using the utility supply stream for Case Study 3 in Fig. 22.

*2.3.3.4. Utility supply streams mass flowrate allocation.* The utility supply streams mass flowrate allocation starts from the demand stream D1, which requires the lowest C/N ratio requirement among the demand streams (Fig. 23a). Utility supply stream mixing was required during targeting demand stream D1 because no closed-loop was formed to enclose the starting and ending point of targeted demand stream D1. So, the supply stream S5, with the highest C/N ratio among the utility supply streams, was required to shift until the ending point of line S4 met with the ending point of line D1.

The $D_x$ and $D_y$ between line S5 and line D1's ending points were calculated as −2.314 and −72.686 t/d via Eq (5) and Eq (6). Thus, the line S5 was shifted 2.314 and 72.686 t/d against the x- and y-axes. The utility line S2 intercepted with shifted line S5 at (1.352, 16.364) and formed a closed-loop indicating that line D1 was satisfied. The utility SCC from starting point of line D1 to the interception point and the shifted line S5 from the interception point to the ending point of line D1 were identified as the mass flowrate used to satisfy the targeted demand stream D1. The MCU and MNU of each utility supply stream satisfying the demand stream D1 were calculated via Eq (8) and Eq (9).

**Table 21**
The mass flowrate of different ES tested for a top gap of Case Study 3.

| External supply | C/N ratio | Starting point ($x_a$, $y_a$) | Ending point ($x_i$, $y_i$) | MF (t/d) | MC (t/d) | MN (t/d) |
|---|---|---|---|---|---|---|
| ES1 (Chicken manure) | 10.6 | (2.272, 50.343) | (3.074, 58.845) | 9.304 | 8.502 | 0.802 |
| ES2 (Vinegar waste) | 22.9 | (2.272, 50.343) | (3.540, 79.368) | 30.292 | 29.025 | 1.268 |
| ES3 (Rice husk) | 103.5 | (2.272, 50.343) | – | – | – | – |

**Table 22**
The mass flowrate status of OWLA and ES supply streams for Case Study 3.

| Supply streams | C/N ratio | Mass flowrate (t/d) | | |
|---|---|---|---|---|
| | | Available (t/d) | Utilised (t/d) | Not utilised (t/d) |
| ES1 (Chicken manure) | 10.6 | N/A | 9.304 | N/A |
| S1 (Dairy manure) | 13.4 | 5 | 5 | 0 |
| S2 (Swine manure) | 15.8 | 10 | 10 | 0 |
| S3 (Kitchen waste) | 20.3 | 20 | 20 | 0 |
| S4 (Rice straw) | 44.1 | 30 | 25.696 | 4.304 |
| S5 (Corn stover) | 54 | 40 | 40 | 0 |

**Table 23**
The mass flowrates of utility supply streams for Case Study 3.

| Utility supply stream | C/N ratio | MF (t/d) | MC (t/d) | MN (t/d) | CMC (t/d) | CMN (t/d) |
|---|---|---|---|---|---|---|
| | | | | | 0 | 0 |
| ES1 (Chicken manure) | 10.6 | 9.304 | 8.502 | 0.802 | 0.802 | 8.502 |
| S1 (Dairy manure) | 13.4 | 5 | 4.653 | 0.347 | 1.149 | 13.155 |
| S2 (Swine manure) | 15.8 | 10 | 9.405 | 0.595 | 1.745 | 22.560 |
| S3 (Kitchen waste) | 20.3 | 20 | 19.061 | 0.939 | 2.684 | 41.621 |
| S4 (Rice straw) | 44.1 | 25.696 | 25.126 | 0.570 | 3.253 | 66.747 |
| S5 (Corn stover) | 54 | 40 | 39.273 | 0.727 | 3.981 | 106.019 |

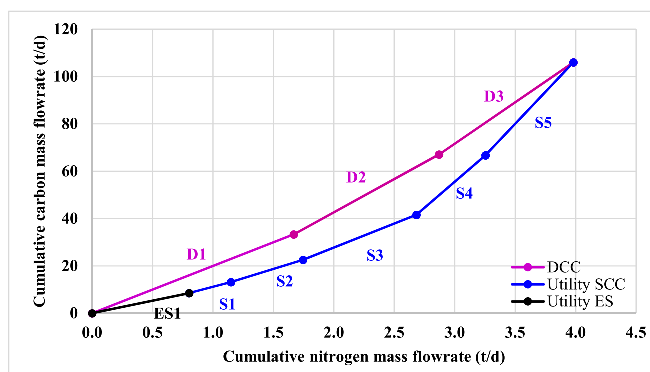


**Fig. 22.** The plot of utility SCC comprised of utility OWLA and ES1 for Case Study 3.

Then, the mass flowrate of shifted line S5 below the interception point and the utility SCC above the interception point was identified as unutilised utility resources. The unutilised utility resources formed a new utility SCC at the subsequent unsatisfied demand stream's starting with the lowest C/N ratio requirement. Similar mass flowrate allocation steps in targeting demand stream D1 were replicated to satisfy the rest of the demand streams (Fig. 23d). The mass flowrate allocations for Case Study 3 are summarised and tabulated in Table 24.

## 3. Conclusion

In this study, the SCC and DCC were formed by introducing cumulative carbon versus cumulative nitrogen mass flowrate as the x- and y-axes of the graphical C/N ratio Pinch Analysis approach, which had not been done before. Series of graphical SCC shifting, namely SCC right-shifting, SCC end-shifting, SCC detaching, and SCC down-shifting, were developed explicitly tackling different supply stream conditions

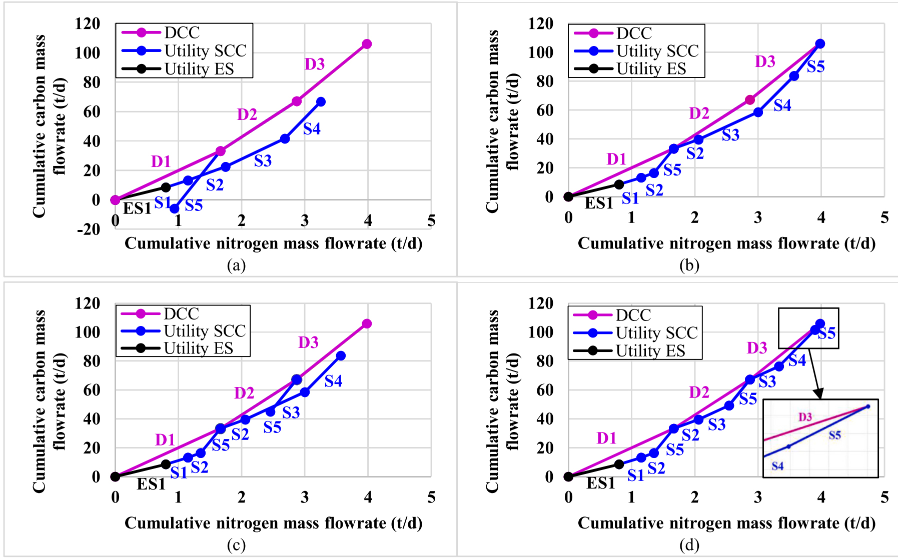


**Fig. 23.** Mass flowrate allocation of utility supply streams for (a and b) Demand 1 (c) Demand 2 (d) Demand 3 in Case Study 3.

**Table 24**
The mass flowrate allocation of utility supply streams for Case Study 3.

| Utility supply stream | Mass flowrate received (t/d) | | |
|---|---|---|---|
| | Demand Stream 1 | Demand Stream 2 | Demand Stream 3 |
| ES1 (Chicken manure) | 9.304 | – | – |
| S1 (Dairy manure) | 5 | – | – |
| S2 (Swine manure) | 3.412 | 6.588 | – |
| S3 (Kitchen waste) | – | 10.222 | 9.778 |
| S4 (Rice straw) | – | 18.191 | 25.696 |
| S5 (Corn stover) | 17.283 | – | 4.526 |

while satisfying the demand streams with the aid of ES. The introduction of heuristics was used to determine the eligible and preferred ES for each of the case studies. Also, the steps to perform resource allocation for each supply stream were developed in this study. Case Study 1 required a total of 48.998 t/d of ES 3 (equivalent to 40.83% of the total mass flowrate of demand streams) mixed with the OWLA to satisfy the demand streams. Case Study 2 required 21.427 t/d of ES 1 (which accounted for 23.81% of the total mass flowrate required by demand streams) mixed with the OWLA to satisfy the demand streams. Case Study 3 required 9.304 t/d (8.46% of total demand mass flowrate) of ES1 mixed with OWLA to satisfy the demand streams. Through the graphical shifting method developed, organic waste can be utilised effectively, and waste in landfills is minimised. These can lead to sustainable biofuel production, conservation of conventional resources and reduced greenhouse gas emission. The results are applicable to target designated biofuels production or equivalent bioprocesses that the production rate is highly dependent on the C/N ratio of the feedstocks. The outcome of this research can further act as guidance for policymakers on sustainable development while drafting the incentive for a supply chain that implements such an integrated design. Besides from mass flowrate allocation of the organic waste resources, logistics is another critical factor during the valorisation of organic waste as it involves transportation expenses and emits an extra carbon footprint on the environment. This study considered a hypothetical case during the targeting of supply and demand streams of the C/N ratio required by the demand streams without considering the distance for biomass transferring which may incur an additional cost and affect the economic feasibility of the proposed solution. Spatial analysis such as allocation of supply and demand streams and detailed economic analysis will be conducted in future studies. The goal of this study is to determine the targets for a feasible design based on the C/N, organic waste available and designated biofuels production. Then, the identified targets could be used to optimise a detailed waste to biofuel supply chain design by accounting for spatial allocation (travel distance) and economic consideration.

## CRediT authorship contribution statement

**Wan Choy Chee:** Writing – original draft, Conceptualization, Methodology. **Wai Shin Ho:** Conceptualization, Methodology, Supervision, Visualization, Investigation, Funding acquisition. **Angel Xin Yee Mah:** Conceptualization, Methodology, Supervision, Visualization, Investigation. **Jiří Jaromír Klemeš:** Conceptualization, Supervision, Writing – review & editing, Funding acquisition. **Yee Van Fan:** Conceptualization, Supervision, Writing – review & editing, Funding acquisition. **Cassendra Phun Chien Bong:** Conceptualization, Supervision, Writing – review & editing. **Keng Yinn Wong:** Conceptualization, Supervision. **Haslenda Hashim:** Conceptualization, Supervision. **Sharifah Rafidah Wan Alwi:** Conceptualization, Supervision. **Zarina Muis:** Conceptualization, Supervision.

## Declaration of competing interest

The authors declare that they have no known competing financial interests or personal relationships that could have appeared to influence the work reported in this paper.

## Acknowledgements

The authors would like to acknowledge the research grants from Universiti Teknologi Malaysia with the grant no. Q.J130000.21A2.05E75, R.J130000.7951.4S150, and R.J130000.7851.5F321, Q.J130000.2851.00L51. Several authors gratefully acknowledged Support from the Grant Agency of the Czech Republic under Project No. 21–45726L in a collaborative bilateral project with the Ministry of Education, Science and Sport of the Republic of Slovenia (project No. 5442–1/2018/106), the Slovenian Research Agency (research core funding No. P2-0412 and P2-0421 and project No. J7-3149).

## References


Alwi, S.R.W., Manan, Z.A., 2007. Targeting multiple water utilities using composite curves. Ind. Eng. Chem. Res. 46 (18), 5968–5976. https://doi.org/10.1021/ie061238k.

Beniche, I., Hungría, J., el Bari, H., Siles, J.A., Chica, A.F., Martín, M.A., 2020. Effects of C/N ratio on anaerobic co-digestion of cabbage, cauliflower, and restaurant food waste. Biomass Conversion and Biorefinery. https://doi.org/10.1007/s13399-020-00733-x.

Black, J.L., Davison, T.M., Box, I., 2021. Methane emissions from ruminants in Australia: mitigation potential and applicability of mitigation strategies. Animals 11 (4), 1–20.

Chin, H.H., Liew, P.Y., Varbanov, P.S., Klemeš, J.J., 2021. Extension of Pinch Analysis to targeting and synthesis of water recycling networks with multiple contaminants. Chem. Eng. Sci. 248, 117223 https://doi.org/10.1016/j.ces.2021.117223. Part B.

Ding, L., Cheng, J., Xia, A., Jacob, A., Voelklein, M., Murphy, J.D., 2016. Co-generation of biohydrogen and biomethane through two-stage batch co-fermentation of macro- and micro-algal biomass. Bioresour. Technol. 218, 224–231. https://doi.org/10.1016/j.biortech.2016.06.092.

Flower, J.R., Linnhoff, B., 1979. Thermodynamic analysis in the design of process networks. Comput. Chem. Eng. 1, 472–486. https://doi.org/10.1016/0098-1354(79)80047-2.

Guo, R., Li, G., Jiang, T., Schuchardt, F., Chen, T., Zhao, Y., Shen, Y., 2012. Effect of aeration rate, C/N ratio and moisture content on the stability and maturity of compost. Bioresour. Technol. 112, 171–178. https://doi.org/10.1016/j.biortech.2012.02.099.

Hills, D.J., 1979. Effects of carbon: nitrogen ratio on anaerobic digestion of dairy manure. Agric. Wastes 1 (4), 267–278. https://doi.org/10.1016/0141-4607(79)90011-8.

Ho, W.S., Khor, C.S., Hashim, H., Macchietto, S., Klemeš, J.J., 2014a. SAHPPA: a novel power pinch analysis approach for the design of off-grid hybrid energy systems. Clean Technol. Environ. Policy 16 (5), 957–970. https://doi.org/10.1007/s10098-013-0700-9.

Ho, W.S., Tohid, M.Z.W.M., Hashim, H., Muis, Z.A., 2014b. Electric system cascade analysis (ESCA): solar PV system. Int. J. Electr. Power Energy Syst. 54, 481–486. https://doi.org/10.1016/j.ijepes.2013.07.007.

Jia, X., Klemeš, J.J., Wan Alwi, S.R., Varbanov, P.S., 2020. Regional water resources assessment using water scarcity pinch analysis. Resour. Conserv. Recycl. 157 https://doi.org/10.1016/j.resconrec.2020.104749.

Juul, N., Münster, M., Ravn, H., Söderman, M.L., 2013. Challenges when performing economic optimisation of waste treatment: a review. Waste Manag. 33 (9), 1918–1925. https://doi.org/10.1016/j.wasman.2013.04.015.

Klemeš, J., Dhole, V.R., Raissi, K., Perry, S.J., Puigjaner, L., 1997. Targeting and design methodology for reduction of fuel, power and $CO_2$ on total sites. Appl. Therm. Eng. 17 (Nos 8–10), 993–1003.

Klemeš, J.J., Varbanov, P.S., Wan Alwi, S.R., Abdul Manan, Z., 2014. Process Integration and Intensification: Saving Energy, Water and Resources, Series. De Gruyter Textbook, De Gruyter, Berlin, Germany, p. 254 (ps).

Klemeš, J.J., Varbanov, P.S., Wan Alwi, S.R., Abdul Manan, Z., 2018a. Process Integration and Intensification: Saving Energy, Water and Resources, 2nd extended edition. De Gruyter Textbook, De Gruyter, Berlin, Germany. Series.

Klemeš, J.J., Varbanov, P.V., Walmsley, T.G., Jia, X.X., 2018b. New directions in the implementation of pinch methodology (PM). Renew. Sustain. Energy Rev. 98, 439–468.

Klemeš, J.J. (Ed.), 2022. Handbook of Process Integration (PI): Minimisation of Energy and Water Use, Waste and Emissions, 2nd updated edition. Elsevier/Woodhead Publishing, Cambridge, UK. ISBN 978-0-21-823850-9.

Li, Y., Zhang, R., Liu, G., Chen, C., He, Y., Liu, X., 2013. Comparison of methane production potential, biodegradability, and kinetics of different organic substrates. Bioresour. Technol. 149, 565–569. https://doi.org/10.1016/j.biortech.2013.09.063.

Li, Z., Chen, Z., Ye, H., Wang, Y., Luo, W., Chang, J.S., Li, Q., He, N., 2018. Anaerobic co-digestion of sewage sludge and food waste for hydrogen and VFA production with microbial community analysis. Waste Manag. 78, 789–799. https://doi.org/10.1016/j.wasman.2018.06.046.

Linnhoff, B., Flower, J.R., 1978. Synthesis of heat exchanger networks. AIChE 24 (4), 633–642.

Linnhoff, B., Hindmarsh, E., 1983. The pinch design method for heat exchanger networks. Chem. Eng. Sci. 38 (5), 745–763. https://doi.org/10.4028/www.scientific.net/AMR.512-515.1253.

Liu, W.H., Kaliappan, K., Wan Alwi, S.R., Lim, J.S., Ho, W.S., 2016. Power Pinch Analysis supply side management: strategy on purchasing and selling of electricity. Clean Technol. Environ. Policy 18 (8), 2401–2418. https://doi.org/10.1007/s10098-016-1213-0.

Manikandan, K., Viruthagiri, T., 2010. Optimisation of C/N ratio of the medium and fermentation conditions of ethanol production from tapioca starch using co - culture of aspergillus Niger and sachormyces cerevisiae. Int. J. ChemTech. Res. 2 (2), 947–955.

Rawoof, S.A.A., Kumar, P.S., Vo, D.V.N., Subramanian, S., 2021. Sequential production of hydrogen and methane by anaerobic digestion of organic wastes: a review. In: Environmental Chemistry Letters, 19. Springer Science and Business Media Deutschland GmbH, pp. 1043–1063. https://doi.org/10.1007/s10311-020-01122-6. Issue 2.

Shahbaz, M., Ammar, M., Korai, R.M., Ahmad, N., Ali, A., Khalid, M.S., Zou, D., Li, X., 2020. Impact of C/N ratios and organic loading rates of paper, cardboard and tissue wastes in batch and CSTR anaerobic digestion with food waste on their biogas production and digester stability. SN Appl. Sci. 2 (8) https://doi.org/10.1007/s42452-020-03232-w.

Shahbaz, M., Ammar, M., Zou, D., Korai, R.M., Li, X.J., 2019. An insight into the anaerobic Co-digestion of municipal solid waste and food waste: influence of Co-substrate mixture ratio and substrate to inoculum ratio on biogas production. Appl. Biochem. Biotechnol. 187 (4), 1356–1370. https://doi.org/10.1007/s12010-018-2891-3.

Skouteris, G., Ouki, S., Foo, D., Saroj, D., Altini, M., Melidis, P., Cowley, B., Ells, G., Palmer, S., O'Dell, S., 2018. Water footprint and water pinch analysis techniques for sustainable water management in the brick-manufacturing industry. J. Clean. Prod. 172, 786–794. https://doi.org/10.1016/j.jclepro.2017.10.213.

Tan, R.R., Aviso, K.B., Foo, D.C.Y., 2018. Carbon emissions pinch analysis of economic systems. J. Clean. Prod. 182, 863–871. https://doi.org/10.1016/j.jclepro.2018.02.082.

Tanimu, M.I., Ghazi, T.I.M., Harun, R.M., Idris, A., 2014. Effect of carbon to nitrogen ratio of food waste on biogas methane production in a batch mesophilic anaerobic digester, 5, pp. 5–8. https://doi.org/10.7763/IJIMT.2014.V5.497, 2.

Wang, X., Yang, G., Feng, Y., Ren, G., Han, X., 2012. Optimising feeding composition and carbon-nitrogen ratios for improved methane yield during anaerobic co-digestion of dairy, chicken manure and wheat straw. Bioresour. Technol. 120, 78–83. https://doi.org/10.1016/j.biortech.2012.06.058.

Yong, Z., Dong, Y., Zhang, X., Tan, T., 2015. Anaerobic co-digestion of food waste and straw for biogas production. Renew. Energy 78, 527–530. https://doi.org/10.1016/j.renene.2015.01.033.

Zhang, C., Xiao, G., Peng, L., Su, H., Tan, T., 2013. The anaerobic co-digestion of food waste and cattle manure. Bioresour. Technol. 129, 170–176. https://doi.org/10.1016/j.biortech.2012.10.138.

Zhong, W., Chi, L., Luo, Y., Zhang, Z., Zhang, Z., Wu, W.M., 2013. Enhanced methane production from Taihu Lake blue algae by anaerobic co-digestion with corn straw in continuous feed digesters. Bioresour. Technol. 134, 264–270. https://doi.org/10.1016/j.biortech.2013.02.060.